nature nanotechnology

SUPPLEMENTARY INFORMATION

https://doi.org/10.1038/s41565-020-0723-4

In the format provided by the authors and unedited.

Engineering synthetic breath biomarkers for respiratory disease

Leslie W. Chan[1], Melodi N. Anahtar[1,2], Ta-Hsuan Ong[3], Kelsey E. Hern[2], Roderick R. Kunz[3] and Sangeeta N. Bhatia[1,2,4,5,6,7] ✉

[1]Koch Institute for Integrative Cancer Research, Massachusetts Institute of Technology, Cambridge, MA, USA. [2]Harvard–MIT Division of Health Sciences and Technology, Institute for Medical Engineering and Science, Massachusetts Institute of Technology, Cambridge, MA, USA. [3]Biological and Chemical Technologies Group, Massachusetts Institute of Technology Lincoln Laboratory, Lexington, MA, USA. [4]Department of Electrical Engineering and Computer Science, Massachusetts Institute of Technology, Cambridge, MA, USA. [5]Department of Medicine, Brigham and Women's Hospital, Harvard Medical School, Boston, MA, USA. [6]Broad Institute, Massachusetts Institute of Technology and Harvard, Cambridge, MA, USA. [7]Howard Hughes Medical Institute, Cambridge, MA, USA. ✉e-mail: sbhatia@mit.edu

Volatile-releasing nanosensors of in vivo protease activity enable breath-based monitoring of respiratory disease

Leslie W. Chan[1], Melodi N. Anahtar[1,2], Ta-Hsuan Ong[3], Kelsey E. Hern[2], Roderick R. Kunz[3], Sangeeta N. Bhatia[1-2, 4-7]*

Table of Contents

Supplementary Text

Description of pharmacologically based pharmacokinetic (PBPK) model for vABNs

To predict the effects of key parameters (i.e. protease concentration, vABN dosing, vABN cleavage kinetics, and reporter partitioning) on reporter concentration in exhaled breath, we constructed a mathematical model for *in vivo* vABN and freed reporter behavior. Mathematical models have been previously developed to track ABN distribution and predict reporter concentrations in urine.[1,2] Given the novelty of our breath-based readout, we created a new mathematical model that draws upon the kinetic principles of our previous models while incorporating transport throughout the respiratory tract. In this model, we tracked vABN transport and subsequent activity in three main compartments: (1) the pulmonary lumen, which is composed of air, (2) the pulmonary tissue, and (3) the breath collection chamber, which in this case is the 100cc syringe housing the mouse.

In this model, we tracked vABN transport and activity in three main regions: (1) the pulmonary lumen, which is made up of air, (2) the pulmonary tissue, which is the region where the vABNs come in contact with NE, and (3) the breath collection chamber, which in this case is the syringe that the mice are enclosed in.

Compartment 1: vABN absorption from the lung lumen

In this model, the lung lumen is considered the air space of the lungs and can be represented as the tidal volume. Because we deliver the vABNs into the lungs via intratracheal instillation, we assume that the entire dose is present in the lumen at *t=0*. Once in the lumen, the vABNs can penetrate into the underlying pulmonary tissue at a rate that we define as k_{Tissue}^{NP}.

$$\frac{dC_{lumen}^{NP}}{dt} = -k_{tissue}^{NP}(C_{lumen}^{NP} - C_{tissue}^{NP}) \quad \text{[S1]}$$

Compartment 2: vABN clearance from the pulmonary tissue

In our model, we have grouped the epithelial lining fluid (ELF), the alveolar macrophages within that fluid, and the underlying lung epithelium into a compartment that we refer to as the “pulmonary tissue”. The concentration of the vABNs in the tissue is influenced by cleavage by target proteases (NE), non-specific cleavage by other proteases (N.S.), and phagocytosis by alveolar macrophages in the ELF. PEG polymers larger than 20 kDa have been shown to have high retention rates in pulmonary tissue at early timepoints after intratracheal administration[3]. Since we are only modeling up to 3 hours after dosing, our model does not account for transport from the pulmonary tissue into systemic circulation.

$$\frac{dC_{tissue}^{NP}}{dt} = k_{tissue}^{NP}(C_{lumen}^{NP} - C_{tissue}^{NP}) - k_{phago}^{NP}C_{tissue}^{NP} - \frac{k_{cat}^{NE}\,[NE]\,C_{tissue}^{NP}}{K_m^{NE}+C_{tissue}^{NP}} - \frac{k_{cat}^{N.S.}\,[N.S.]\,C_{tissue}^{NP}}{K_m^{N.S.}+C_{tissue}^{NP}} \quad \text{[S2]}$$

vABN cleavage is modeled using Michaelis-Menten enzyme kinetics. The kinetic terms describing cleavage by NE (k_{cat}^{NE} and K_m^{NE}) were determined through *in vitro* experiments, as described in the main text, while the terms for non-specific enzyme degradation ($k_{cat}^{N.S.}$ and $K_m^{N.S.}$) were fit to *in vivo* data (see below) and assumed to be the same for all vABNs, regardless of their reporter.

To obtain the concentration of NE in the ELF, we performed bronchoalveolar lavage fluid (BALF) in PA01 infected mice using a single wash (1 mL PBS instilled, with approximately 80% aspirated). The collected fluid was centrifuged to remove cells in the ELF, and the supernatant NE concentration was measured via ELISA. To correct for NE dilution in BALF, we normalized this measured concentration, 5.29 ng/mL, to the total volume of ELF in the lungs, which is where NE would be present. Using an ELF volume of 40 µL[4,5], we estimated an NE concentration of 3.5 nM.

$$\left(5.29\,\frac{ng}{mL} of\ NE\ in\ BALF\right)(0.8\,mL\ of\ BALF) = \left(x\,\frac{ng}{mL}\right)(0.04\,mL\ of\ ELF), x = 105.8\,\frac{ng}{mL} \quad [S4]$$

$$105.8\,\frac{ng}{mL} * \frac{1e3\ mL}{1\ L} * \frac{1\ g}{1e9\ ng} * \frac{1\ mol}{29.5e3\ g} * \frac{1e9\ nmol}{1\ mol} = 3.5\ nM\ NE \quad [S5]$$

Compartment 3: Transport of liberated VOC reporters through the pulmonary tissue

Once the vABNs are cleaved, the liberated reporters can either diffuse from the tissue into the lumen ($k_{tissue}^{reporter}$), which allows them to be exhaled into the chamber, or transported into the blood ($k_{clear}^{reporter}$), after which they are assumed to be diluted in the blood volume and unavailable for exhalation.

$$\frac{dC_{tissue}^{reporter}}{dt} = -k_{tissue}^{reporter}\left(\frac{C_{tissue}^{reporter}}{H_{t:a}} - C_{lumen}^{reporter}\right) - k_{clear}^{reporter} * \frac{C_{tissue}^{reporter}}{H_{t:b}^{reporter}} + \frac{k_{cat}^{NE}\,[NE]\,C_{tissue}^{NP}}{K_m^{NE}+C_{tissue}^{NP}} + \frac{k_{cat}^{N.S.}\,[N.S.]\,C_{tissue}^{NP}}{K_m^{N.S.}+C_{tissue}^{NP}} \quad [S6]$$

The clearance rate of reporters from the respiratory tissue into blood ($k_{clear}^{reporter}$) was fit to empirical values shown in **Fig. 3f** and assumed to be equal for all reporters due to their similar MWs. $H_{t:a}$ is the tissue:air partition coefficient, which represents the ratio of the VOC reporter concentration in the tissue to the concentration in air. A higher $H_{t:a}$ implies that the reporter partitions more readily into tissue. Similarly, the $H_{b:a}$ represents the ratio of the VOC reporter concentration in the blood to the concentration in air. The $H_{t:b}$ (tissue:blood partition coefficient) was calculated by dividing $H_{t:a}^{VOC}$ by $H_{b:a}^{VOC}$, as is standard for physiologically based pharmacokinetic modeling. The $H_{t:a}^{VOC}$ and $H_{b:a}^{VOC}$ were measured *in vitro* for each reporter except PFC7, which was assumed to have the same partition coefficients as PFC5 (see Methods in the main text).

Compartment 4: VOC reporter concentration in the pulmonary lumen

The reporters that diffuse from the tissue and into the lung lumen are represented by the following equation:

$$\frac{dC_{lumen}^{reporter}}{dt} = k_{tissue}^{reporter}\left(\frac{C_{tissue}^{reporter}}{H_{t:a}} - C_{lumen}^{reporter}\right) - Q_{m,c}\left(C_{lumen}^{reporter} - C_{chamber}^{reporter}\right) \quad [S7]$$

The first term of Eq. S7 describes the diffusion of the VOC reporter between the lumen and tissue. The second term describes the movement of the reporter that is influenced by breathing. Q_m represents the minute volume, which is the volume of gas that is inhaled or exhaled per minute. Minute volume consists of both the alveolar volume (the volume of air that undergoes gas exchange) and the dead space (air that is not perfused). The value for Q_m is typically given in units of L/min. To correct for the units, the term $Q_{m,c}$ was used, whereby Q_m is divided by tidal volume (the volume of air displaced between inhalation and exhalation). With this correction, $Q_{m,c}$ effectively represents the ventilation rate.

Compartment 5: The breath collection chamber

Finally, the chamber compartment represents the receptable that is used to collect breath. In the model, this compartment is the syringe that encloses mice during breath collection. In humans, it could represent any collection container that the patient breathes in and out of during breath collection. The reporters in the lumen that do not diffuse back into the pulmonary tissue are exhaled into the chamber. Assuming ideal transport of VOCs into and out of the lumen, the chamber concentration can be modeled as:

$$\frac{dC_{chamber}^{reporter}}{dt} = Q_{m,c}\left(C_{lumen}^{reporter} - C_{chamber}^{reporter}\right) \quad [S8]$$

Furthermore, this equation accounts for VOC reporters in the chamber that are re-inhaled, which affects the concentration of reporters in the collected breath.

ppb conversion

All concentrations in the model are in terms of μM. To convert the final exhaled concentrations into *ppb*, the following conversion factor was used:

$$Exh_{ppm} = C_{chamber}^{reporter} * 1e-6 * 1000 * 24450 \quad [S9]$$

$$Exh_{ppb} = Exh_{ppm} * 1000 \quad [S10]$$

Parameter estimation

Any values that were not measured or available in the literature were determined by fitting the model for PFC1 to *in vivo* breath data obtained from administration of 100 μM of the NE responsive HFA1-vABN into infected mice (data shown in Fig. 3f of the main text). The MATLAB function *lsqcurvefit* was used to simultaneously fit $k_{tissue}^{reporter}$, $k_{clear}^{reporter}$, $k_{cat}^{N.S.}$, and $K_m^{N.S.}$ until a local minimum was reached. The fit was bound by the constraints that all values must be positive. k_{tissue}^{NP} was manually adjusted to obtain a value that was less than $k_{tissue}^{reporter}$ and within a range of previously modeled values[2]. The fitted values for $k_{cat}^{N.S.}$, and $K_m^{N.S.}$ were then compared to the measured values of k_{cat}^{NE}, and K_m^{NE} for HFA1, and scaled accordingly to obtain a more generalized form that could be used to account for the differences in cleavage rate for vABNs with other HFA reporters. The *[N.S.]* was held constant throughout all ABN models, as the concentration of nonspecific enzymes should not change based on the vABN.

	Parameter	Description	Unit	Value	Source
Flow rates	Q_m	Minute volume	L/min	0.037	[6]
	$Q_{m,c}$	Corrected minute volume	1/min	$\frac{Q_m}{V_{tidal}}$	Estimate
Volumes	V_{tidal}	Tidal volume	mL	0.131	[6]
Partition coefficients	$H_{b:a}^{reporter}$	VOC reporter blood:air partition coefficient	-	PFC1: 65.16 PFC3: 20.06 PFC5: 25.63	Measurement
	$H_{t:a}^{reporter}$	VOC reporter tissue:air partition coefficient	-	PFC1: 57.64 PFC3: 137.24 PFC5: 58.89	Measurement
	$H_{t:b}^{reporter}$	VOC reporter tissue:blood partition coefficient	-	$\frac{H_{t:a}^{reporter}}{H_{b:a}^{reporter}}$	Defined
Clearance rates	k_{tissue}^{NP}	Diffusion rate of the vABNs into tissue	1/min	0.05	Manually fit to *in vivo* data
	k_{phago}^{NP}	Clearance rate of vABNs via macrophages	1/min	0.0006	[2]

	$k_{tissue}^{reporter}$	Diffusion rate of VOC reporters into tissue	1/min	39.9	Computationally fit to *in vivo* data
	$k_{clear}^{reporter}$	Clearance rate of VOC reporters into blood	1/min	22.1	Computationally fit to *in vivo* data
Michaelis-Menten Kinetics	*[NE]*	NE concentration in the respiratory tissue	nM	3.5	Measurement
	k_{cat}^{NE}	Turnover number for NE	1/min	PFC1: 186 PFC3: 204.0 PFC5: 166.8 PFC7: 4.2	Measurement
	K_m^{NE}	Michaelis constant for NE	μM	PFC1: 10.91 PFC3: 11.98 PFC5: 66.78 PFC7: 22.34	Measurement
	[N.S.]	Concentration of nonspecific enzymes in the respiratory tissue	μM	3.82	Computationally fit to *in vivo* data
	$k_{cat}^{N.S.}$	Turnover number for nonspecific enzymes	1/min	k_{cat}^{NE} / 73.6	Computationally fit to *in vivo* data
	$K_m^{N.S.}$	Michaelis constant for nonspecific enzymes	μM	$K_m^{NE} * 33.7$	Computationally fit to *in vivo* data

Prediction of Human Breath Signal

We can use our PBPK model for allometric scaling to predict breath signal in humans. The model parameters that differ the most significantly between mice and humans are: (1) the vABN dose, (2) the minute and tidal volumes, (3) the NE concentration in the infected lungs, (4) the concentration of nonspecific enzymes in the respiratory tissue. Based on prior literature, we assume that the partition coefficients hold across species (Aldo 2012). We assume that the macrophage phagocytosis rate is the same in mice and humans. We can also use the catalytic rate constants (k_{cat}) and Michaelis-Menten constants (K_m) that we obtained *in vitro*, as they were calculated using human NE.

(1) The vABN dose: Following guidelines outlined by the FDA and the literature, we can scale the dose across species by calculating the *Human Equivalent Dose* (*HED*) of the vABNs by using the following equation:

$$HED\ (mg\ /\ kg)\ =\ Animal\ dose\ (mg\ /\ kg)\ \times\ (\frac{Animal\ k_m}{Human\ k_m})$$

where k_m (not to be confused with the Michaelis Menten constant, K_m) is an established correction factor for each species that is based on body weight and surface area (Nair 2016, FDA 2005). For our mouse studies, we administered 10 uM of vABN by peptide concentration in 50 µL of PBS, making our dose in a 30-g mouse the following:

50e-6L * 10e-6 mol/L * 2183.6 g/mol * 1e6 µg/ 1g * 1/0.03 kg = 36.4 µg/kg (mouse)

Based on FDA guidelines, the k_m for humans and mice are 37 and 3, respectively. Using the *HED* equation above, the human equivalent dose is:

36.4 µg/kg * (3/37) = 2.95 µg/kg (human)

If we were to deliver this dose by diluting it in 3 mL of saline, which is the saline volume commonly used to administer the adult dose of nebulized albuterol, the starting dose in a 60-kg human would be:

60 kg * 2.951 µg/kg * 1e-6g/µg * 1/2183.6 mol/g * 1/0.003L * 1e6 umol/mol = 27.03 µM (human)

This vABN dose concentration is 2.7 times higher than our current concentration and falls within the concentration range for which acute toxicity was not observed.

(2) The minute and tidal volumes: The minute volume is the volume of air that is moved in and out of the lungs per minute, while the tidal volume is the volume of air displaced between inhalation and exhalation (Levitsky 2018). The average minute volume for humans is 7.5 L/min, which is 200 times greater than mice (Arms 1988). The tidal volume for a human can be calculated using an established allometric equation $Y = aM^b$, where *a* and *b* are established constants specific to the organism (for humans, $a = 7.69$ and $b = 1.04$) and M is the mass of the organism in kg (Derelanko). Using this equation, the tidal volume for a 60 kg human is 543.5 mL, which aligns with the 500 mL approximation that is often cited in literature (Levitsky 2018). This is 4000 times greater than mice. Significantly larger human lung volumes could produce greater reporter

abundance, but also dilute reporter concentration in breath. The PBPK model factors in this dilution to predict the final breath signal.

(3) NE concentration in an infected human: A prior study found that NE concentration in bronchoalveolar lavage fluid (BALF) from 9 patients with lung infection averaged 780.5 µg/L (26.4 nM) (Lengas 1994). BALF was collected by instilling 80-100 mL of saline solution into the lung regions where consolidation was noted on a chest X-ray. Therefore, BALF concentrations are diluted relative to actual concentrations in the epithelial lining fluid (ELF). To estimate the actual NE concentration in ELF (the concentration to which vABNs are exposed), the following figures were used: (1) during BALF collection, average fluid recovery was 47% of the instilled saline solution (Lengas 1994) and (2) in humans, ~1 mL of epithelial lining fluid (ELF) is recovered per 100 mL of lavage fluid [7]. Therefore, in 47 mL of lavage fluid, one would expect 0.47 mL of ELF and the estimated NE concentration in human lungs during infection would be the following:

$$(780.5\ \mu g/L)(47\ mL\ of\ BALF) = (x\ \mu g/L)(0.47\ mL\ of\ ELF)$$

$$x = 78.1\ mg/L\ or\ 2.64\ \mu M\ of\ NE\ in\ infected\ human\ lungs$$

This estimated concentration is on par with other estimates derived using theoretical modeling of quantum proteolysis by human neutrophils (Liou 1995). Furthermore, the 9 patients from whom this value was derived were outpatients, meaning they were not hospitalized for their illness, which implies milder disease within a clinical context (Lengas 1994).

(4) Concentration of nonspecific (N.S.) enzymes in an infected human: Mouse values for N.S. enzyme concentration were derived by fitting the model to empirical data from breath studies in infected mice. Human values would need to be derived in a similar fashion. For the purposes of our estimation of human breath signal, we assumed equivalent N.S. enzyme concentration.

Using the adjusted human values, the PBPK model predicts that the breath signal 10 min after vABN administration in humans during lung infection is ~4.3 fold higher than in healthy humans and ~3.9-fold higher than in infected mice (**Supplementary Fig. 13**). The absolute signal is at ppb concentrations which is within the limit of detection of the mass spectrometer. These predictions support the feasibility of using our platform to monitor neutrophil elastase activity in humans during lung infection. We expect these values to be even more elevated in during lung infection in individuals with AATD given the deficiency in NE inhibition. Furthermore, collection of human breath onto sorbent tubes, a method in which volatiles in liters of breath can be concentrated onto a solid support for subsequent thermal desorption into a VOC detector, can further increase reporter concentrations up to several orders of magnitude to increase testing sensitivity (Lawal 2017).

Code information

The accompanying code can be accessed at https://github.com/NN19092108A/PBPKmodel.
The code was run in MATLAB R2017a.

Supplementary Material and Methods

Nanocarrier distribution study. For immunohistological visualization after intratracheal instillation into the lungs, 40 kDa 8-arm PEG amine was labeled with EZ-Link NHS-Biotin (Thermo Scientific) via an overnight reaction at a 2:1 molar ratio in PBS. Uncoupled NHS-biotin was removed using spin filters (Millipore, 10kDa MWCO). The concentration of biotin in the finished product was quantified using the Quant*Tag Biotin Quantification Kit (Vector Laboratories). 10 µM biotinylated 8-arm PEG was delivered into mice that were infected with PA01 24 h prior. 10 min after intratracheal instillation of the 8-arm PEG, mice were euthanized and their lungs were inflated with 4% PFA and harvested. After overnight fixation in 4% PFA, the lungs were transferred to 70% ethanol and subsequently embedded in paraffin. 5 µm-thick tissue sections were stained for biotin using the streptavidin-HRP ABC kit (Vector Laboratories) with DAB.

Characterization of vABN cleavage by mouse NE. Recombinant mouse NE (rmNE) (R&D Systems 4517-SE-010) was first activated with recombinant mouse cathepsin C (rmCTSC) (R&D Systems 2336-CY). Briefly, a 0.44 mg/mL rmCTSC stock was first mixed 1:1 with 50 mM MES, 50 mM NaCl, 5 mM DTT pH 5.5 buffer for 30 min at RT. rmCTSC was then combined with 0.44 mg/mL rmNE and buffer (50 mM MES, 50 mM NaCl, pH 5.5) at a volumetric ratio of 1:1:4.6. The reaction was incubated for 2h at 37°C for rmNE activation. Activated rmNE was diluted to pM to nM concentrations in a pH 7.5 assay buffer (50 mM Tris, 1 M NaCl, 0.05% (w/v) Brij-35) to assess concentration-dependent release of volatile reporters from vABNs. In this experiment, rmNE and vABN solutions were mixed 1:1 in a 400-µL reaction volume in Exetainers® for the following final concentrations: 10 µM vABNs by peptide concentration and 1, 10, 100 pM, or 1 nM rmNE. Reaction solutions were gently mixed on a shaker for 1h after which 2cc of the reaction headspace was retrieved using a syringe and 25g needle through the Exetainer® septum and immediately injected into the port of a PTR-MS (Ionicon PTR-TOF 1000*Ultra*) for reporter quantification. Reactions with human NE was included for comparison. In a subsequent study, sivelestat was assessed for its ability to prevent volatile release through rmNE inhibition. rmNE was pretreated with sivelestat for 10 min before addition of vABN. Final concentrations in the 400-µL reaction volume were 10 µM vABN by peptide concentration, 20 nM rmNE, and sivelestat in pH 7.5 assay buffer.

***In vitro* cleavage studies in simulated lung fluid (SLF).** vABN cleavage by NE, CTSG, PR3, GZMB, CTSB, CTSD, MMP9, and MMP13 was assessed in Gamble's SLF adjusted to pH 6.5 to mimic the depressed pH in lung fluid during inflammation.[8] SLF was also modified with 100 mg/L DPPC, the most abundant phospholipid in lung surfactant, and was used to dilute protease and vABN stocks. In each reaction, protease and vABN solutions were mixed 1:1 in a 400-µL reaction volume in Exetainers® for the following final concentrations: 0.5 nM protease and 1 µM vABN by peptide concentration. Reactions were gently mixed on a shaker, and released HFA1 reporter in the reaction headspace was measured at 5, 10, 15, 20, 25, and 30 min. 3 cc of reaction headspace was drawn from the Exetainer using a 25g needle and syringe, and the sample was immediately injected into the port of a PTR-MS.

Characterization of reporter levels in the urine headspace. Following intratracheal administration of 10 µM vABNs, 7-8 week old female CD-1 mice were placed in custom housing with a 96-well plate base for 30 min for urine collection. At the end of the 30 min period, mouse

bladders were voided into the plate and all urine was transferred immediately into Exetainers®. Reporter levels in the headspace was quantified by opening Exetainers® at the inlet of a triple quadrupole mass spectrometer for 0.25 min. Breath was collected from the same mice at the usual 10 min timepoint for comparison to reporter levels in the urine headspace.

Control study to verify null HFA1 signal in undosed mice. To confirm absence of HFA1 signal in breath from mice without vABNs, a standard breath study was completed with healthy mice and lung infection models 24 h post-inoculation both with and without 10 µM vABN.

vABN solubility assays in simulated lung fluid (SLF). To assess solubility of vABNs in a simulated lung environment, Cy5-labeled vABNs were diluted to 10 and 100 µM by peptide concentration in modified Gamble's SLF adjusted to pH 7.4. The recipe for Gamble's SLF is 0.095 g/L $MgCl_2$, 6.019 g/L NaCl, 0.298 g/L KCl, 0.126 g/L Na_2HPO_4, 0.063 g/L Na_2SO_4, 0.368 g/L $CaCl_2{\cdot}2H_2O$, 0.574 g/L CH_3COONa, 2.604 g/L $NaHCO_3$, and 0.097 g/L $HOC(COONa)(CH_2COONa)2{\cdot}2H_2O$. 100 mg/L DPPC was added to represent phospholipids secreted into lung surfactant by alveolar type II cells. Cy5 absorbance was monitored in sitting solutions over 24h to determine if vABNs were precipitating out of solution. Briefly, 20 µL volumes were carefully pipetted from sitting solutions to a 384-well plate at each timepoint and read immediately using a platereader.

Animal toxicity studies. 50 µL of 5, 20, 100 µM vABNs were administered into 8-week old CD-1 mice via intratracheal instillation. Lungs were harvested 24 h after dosing and fixed in 10% buffered formalin. Lungs were embedded in paraffin, cut into 5 µm sections, and H&E stained. Stained sections were reviewed by a pathologist blinded to the treatment groups.

NE inhibition studies. A single 5 mg/kg dose of sivelestat sodium (Selleck USA) in 50 µL PBS was administered via intratracheal instillation 15 min before vABN administration and subsequent breath collection to determine contribution of NE activity to breath signal.

Comparison of breath signal from free peptide substrate versus vABNs. Equivalent doses of free peptide substrate and vABN (10 µM by peptide concentration) were administered separately into lung infection models and healthy controls. Breath was collected at t = 2, 4, 6, 8, 10, 20, and 30 min after dosing, and breath samples were analyzed by a triple quadrupole mass spectrometer.

Supplementary Figures

Supplementary Table 1. Chemical names and CAS registry numbers for volatile reporters.

Reporter	Chemical name	CAS registry number
HFA1	2,2,3,3,3-Pentafluoropropylamine	422-03-7
HFA2	2,2,3,3,4,4,4-Heptafluorobutylamine	374-99-2
HFA3	1H,1H-Perfluoropentylamine	355-27-1
HFA5	1H,1H-Perfluoroheptylamine	423-49-4
HFA7	1H,1H-Perfluorononylamine	355-47-5

Supplementary Table 2. Summary of biological variables and results from breath studies. ROC curves were generated using values from healthy controls and infected/LPS-challenged mice to determine ability to classify based on breath signal (reflected in AUROC, where AUROC = 1.0 indicates perfect classification and AUROC = 0.5 indicates random classification). *p*-values reflect comparison to random classifier.

Study	Strain and sample size per group	Gender (F/M)	Age (weeks)	Inflammatory agent	SNR (inflamed/healthy)	AUROC/ *p*-value
Figure 4d (24 h)	CD-1 *n* = 4 or 6	F	7-8	*P. aeruginosa* (PA01)	Range: 1.95-3.20 Mean ± s.d.: 2.52 ± 0.53	1.0 0.0105
Figure 5e	C57BL/6N *n* = 17	F	8-10	*E. coli* LPS	Range: 1.59-3.81 Mean ± s.d.: 2.67 ± 0.61	1.0 <0.0001
Figure 6d	C57BL/6J *n* = 7	M	27-30	*S. enterica* LPS	Range: 1.52-2.82 Mean ± s.d.: 2.05 ± 0.43	1.0 0.0017
Figure 6d	C57BL/6J *Serpina1a-e* knockout *n* = 7 or 8	M	27-30	*S. enterica* LPS	Range: 2.00-2.76 Mean ± s.d. : 2.45 ± 0.26	1.0 0.0012

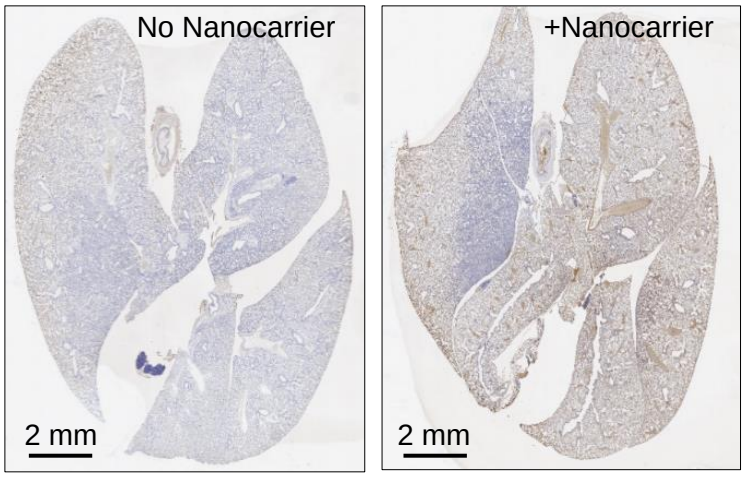

Supplementary Figure 1. Distribution of 8-arm PEG nanocarrier in the infected lung. Lung infection mouse models were administered biotin-labeled 8-arm PEG nanocarrier via IT instillation 24 h after PA01 inoculation and lungs were harvested, fixed, sectioned, and stained for biotin (brown). Whole lung images shown for no nanocarrier control (*n* = 2 mice) and nanocarrier-treated mice (*n* = 3 mice).

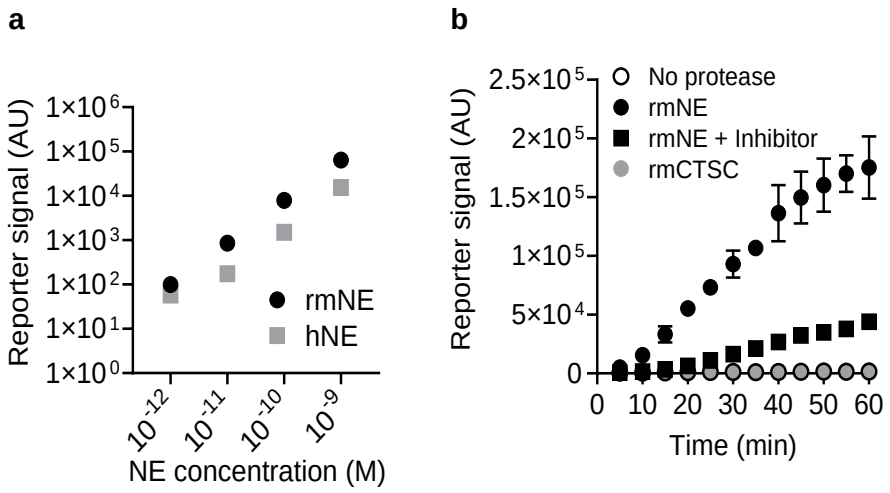

Supplementary Figure 2. Cleavage of vABNs by recombinant mouse NE (rmNE). (**a**) NE concentration-dependent release of volatile reporters from vABNs (mean ± s.d., *n* = 3 independent measurements). Cleavage by human NE (hNE) was included for comparison. (**b**) Inhibition of volatile reporter release using sivelestat, a small molecule NE inhibitor. Recombinant mouse cathepsin C (rmCTSC) was used to activate rmNE and was therefore included as a control (mean ± s.d., *n* = 3 independent measurements). Cleavage experiments were completed independently twice with similar results.

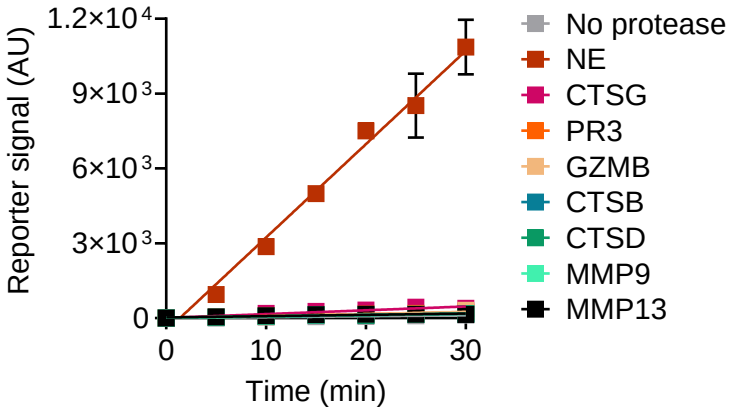

Supplementary Figure 3. Protease cleavage of vABN in pH 6.5 Gamble's simulated lung fluid. 1 µM vABN was reacted with 0.5 nM protease, and PTR-MS was used to measure released HFA1 reporters in the reaction headspace to assess protease specificity (mean ± s.d., *n* = 3 independent measurements).

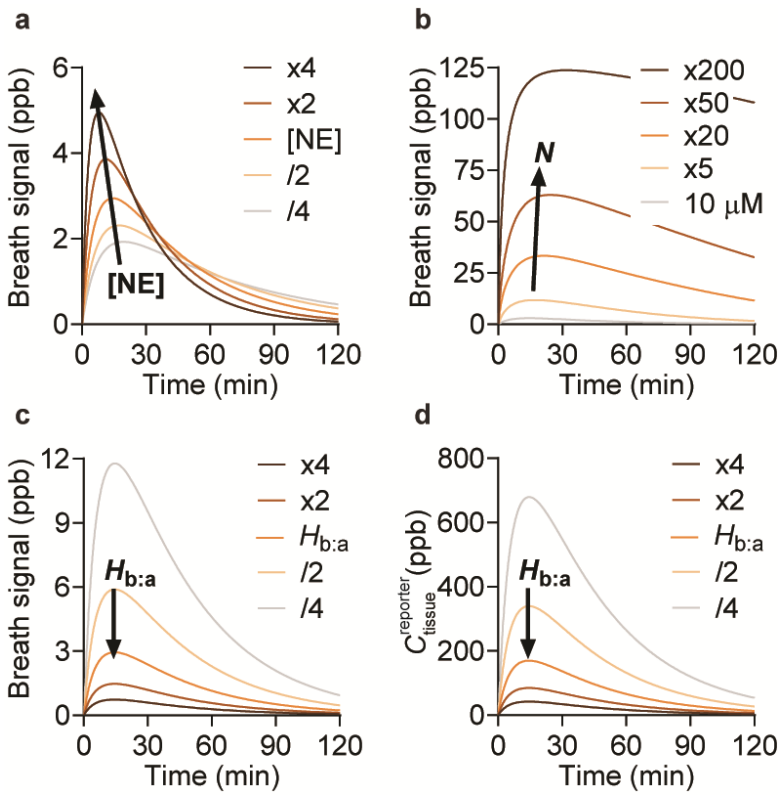

Supplementary Figure 4. Predicted effect of key parameters on breath signal. Key parameters in the PBPK model such as (**a**) NE concentration ([NE]) (**b**) vABN dose (*N*) and (**c**) blood-air partition coefficient of the reporter ($H_{b:a}$) were varied to confirm model functionality. (**a**) At higher [NE], signal curves are narrowed with higher peak breath signal and earlier return of breath signal to baseline, which can be attributed to faster cleavage of the injected vABN dose. (**b**) Micromolar substrate concentration range is predicted to generate breath signal at ppb levels, which is well above the ppt detection limit of mass spectrometry. With increasing vABN dose, we observe increased signal intensity and broadening of signal peaks until a vABN dose is achieved such that even at higher doses, the breath signal remains stable due to establishment of a substrate reservoir. (**c-d**) As $H_{b:a}$ increases, breath signal drops due to reduced reporter concentrations in tissue (i.e. reporters available to partition into air) . Arrows indicate direction of increasing parameter values.

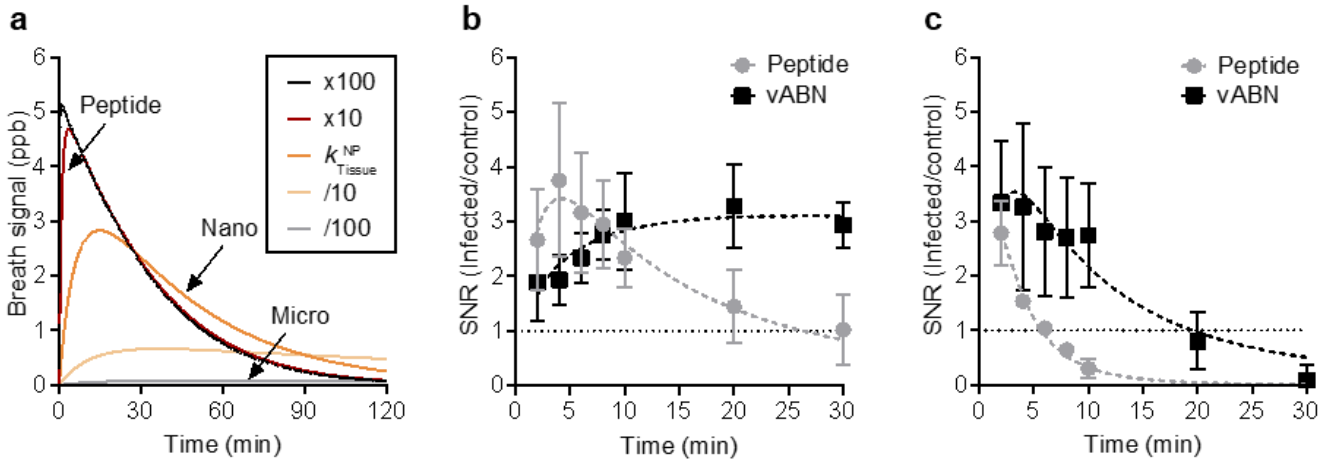

Supplementary Figure 5. Effect of particle size on breath signal. (**a**) PBPK model predictions for breath signal for free peptide substrates and peptide substrates delivered on nano- or microparticle carriers. (**b**) Empirical comparison of breath signal after intrapulmonary delivery of the free peptide substrate versus the nanoformulated peptide substrate (i.e. the vABN) containing the HFA1 reporter (mean ± s.d., *n* = 5 mice per group). (**c**) Empirical comparison of breath signal after intrapulmonary delivery of the free peptide substrate versus vABNs containing the HFA2 reporter (mean ± s.d., *n* = 4 mice per group).

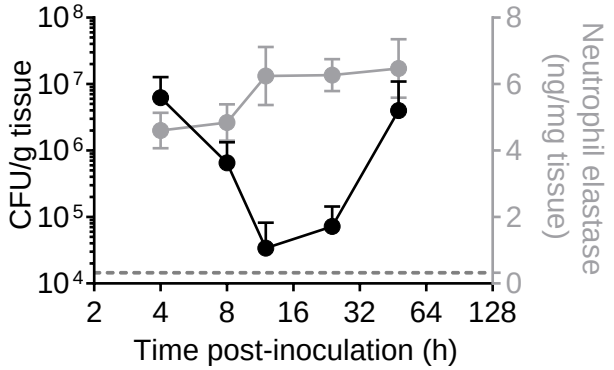

Supplementary Figure 6. Characterization of acute lung infection mouse models. Bacterial burden (black) and neutrophil elastase protein levels (grey) in the lungs of 8-wk old CD-1 mice inoculated with 1.5 x 10^6 cfu PA01 (mean ± s.d., *n* = 3 mice per timepoint). Baseline neutrophil elastase protein level indicated by dotted line.

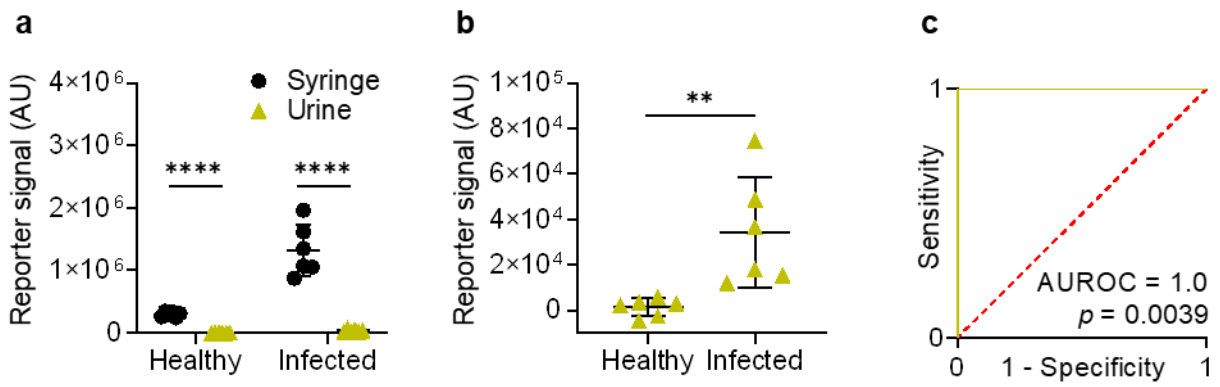

Supplementary Figure 7. Contribution of reporter signal from urine in collected breath samples. As the whole mouse is placed inside the breath collection chamber consisting of a 100cc syringe, control experiments were completed to verify that reporter signal from other sources such as urine contribute minimally to measured reporter signal in the syringe headspace. Urinary reporter signal is possible if freed reporters partition from the lungs into blood circulation and are subsequently cleared by the kidneys. (**a**) Comparison of reporter signal from the urine headspace (cumulative signal from 0-30 min after vABN dosing) versus signal in the syringe headspace (signal from single 10-min timepoint after vABN dosing) (mean ± s.d., n = 6 mice per group, two-tailed t-test, ****$p < 0.0001$). (**b**) Reporter signal from the urine headspace graphed on a magnified y-axis for direct comparison between healthy and infected mice (mean ± s.d., n = 6 mice per group, two-tailed t-test, **$p = 0.0083$). (**c**) ROC curve showing robust distinction between healthy controls and infected mice using reporter signal from the urine headspace shown in ***b*** (n = 6 mice per group, p-value derived from comparison to a random classifier represented by the dashed red line).

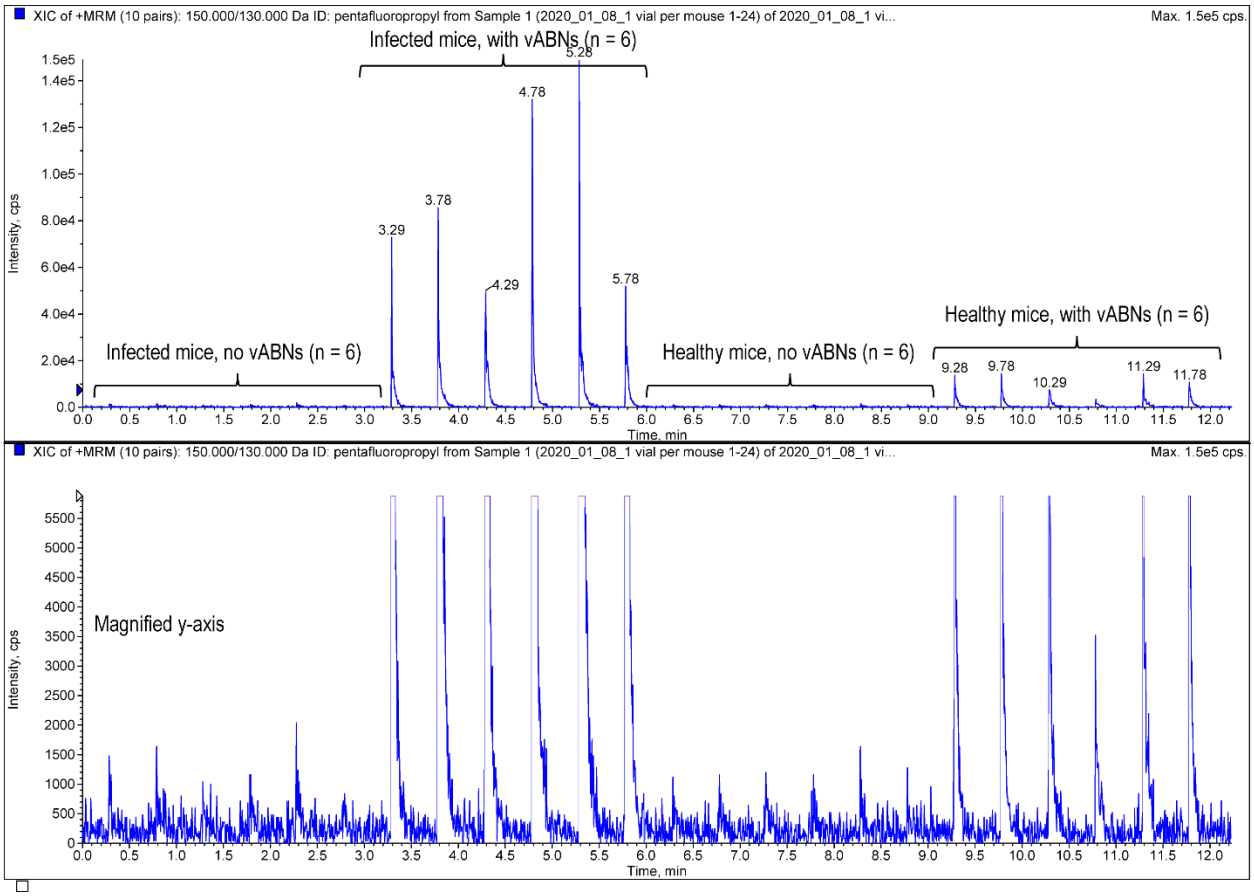

Supplementary Figure 8. Mass spectra confirming no HFA1 background signal in the absence of vABN administration. Each peak represents the reporter signal in breath collected from one mouse. Each sample was analyzed by the mass spectrometer for a duration of 0.25 min.

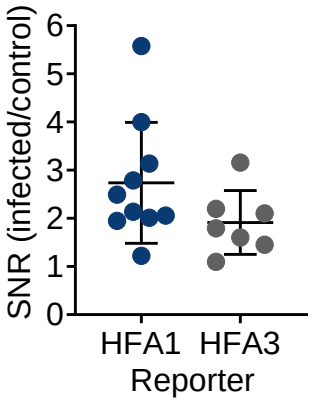

Supplementary Figure 9. Comparison of SNR for vABNs with HFA1 versus HFA3 reporter. SNR was determined using breath signal 10 min after delivery of 10 µM vABN (mean ± s.d., *n* = 7 or 10 mice per group).

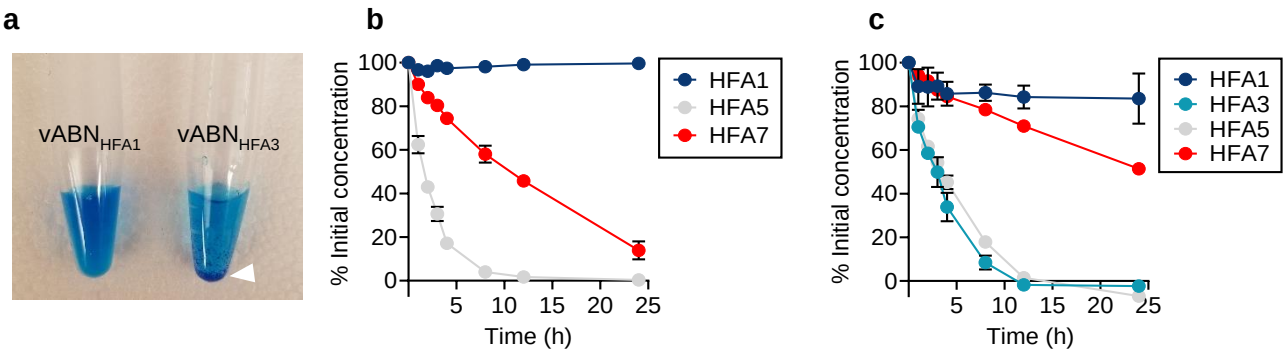

Supplementary Figure 10. vABN stability in simulated lung fluid (SLF). (**a**) Image showing 100 µM solutions of vABNs with HFA1 (left) or HFA3 (right) in SLF. vABNs with HFA3 reporters precipitated immediately during sample preparation (white arrow). Stability of the remaining vABNs were assessed by monitoring Cy5 absorbance in (**b**) 100 µM and (**c**) 10 µM solutions periodically over 24 h (*n* = 3 independent samples per group). (**b**) >99% of HFA1-containing vABNs remained in solution for up to 24h after sample preparation. HFA5- and HFA7-containing vABNs were unstable, with 38% and 10% precipitating out of solution, respectively, within the first hour after sample preparation. (**c**) Similar trends were observed at 10 µM concentration.

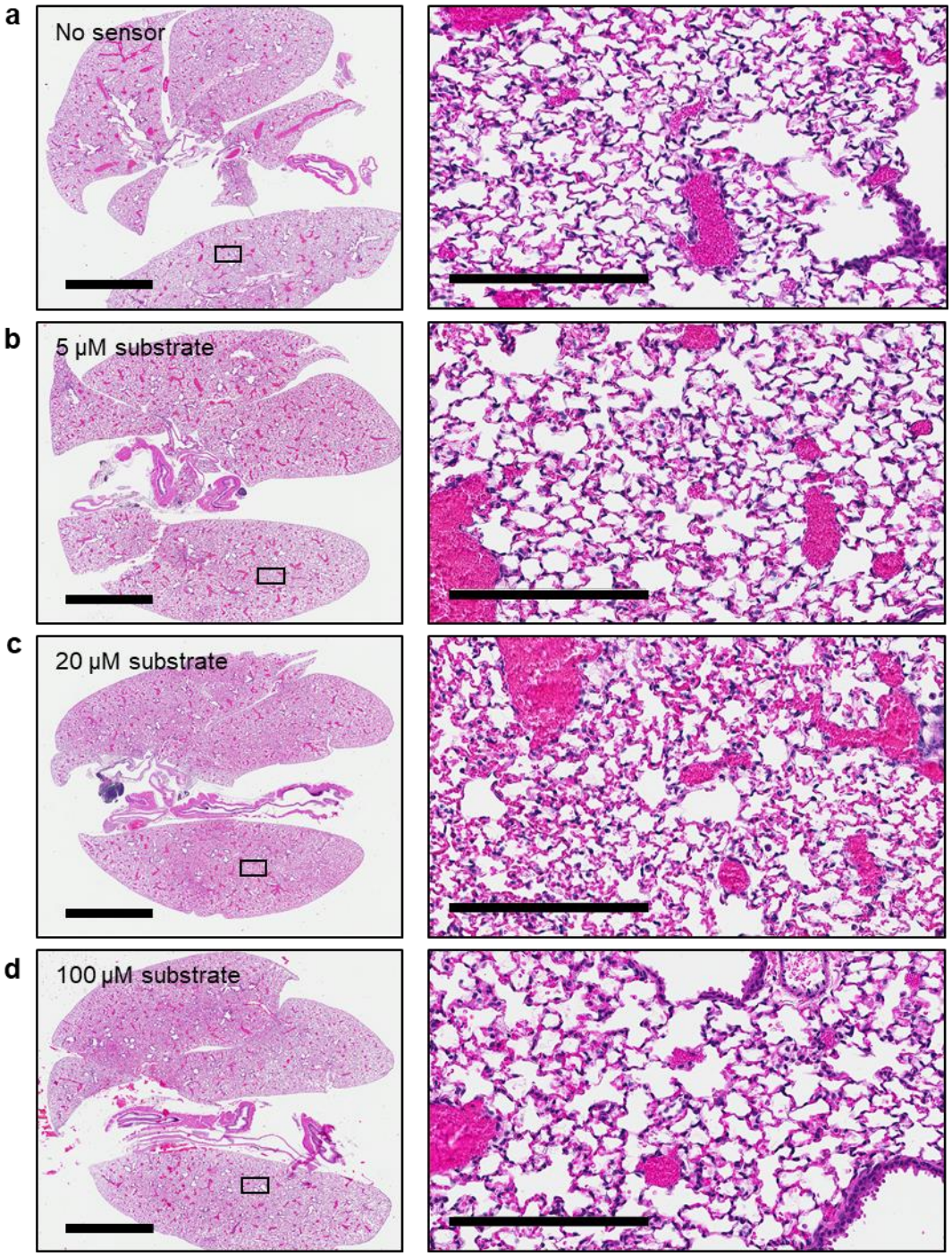

Supplementary Figure 11. vABN biocompatibility. H&E-stained lung tissue sections from CD-1 mice administered (a) no nanosensors or a vABN dose equivalent to (b) 5 µM (c) 20 µM and (d) 100 µM peptide substrate. Images in the left column depict the whole lung (scalebar, 3 mm) and images in the right column depict the area indicated by the rectangle at higher magnification (scalebar, 200 µm) (*N* = 1 independent experiment, *n* = 3 mice per group).

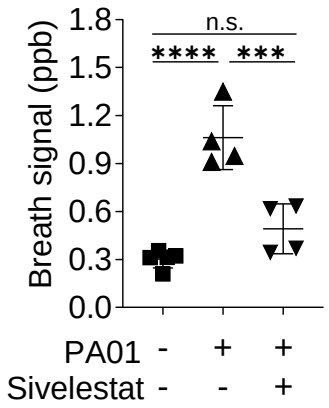

Supplementary Figure 12. Breath signal is specifically driven by neutrophil elastase activity. Breath signal 10 min after vABN administration in healthy controls and lung infection models established using *P. aeruginosa* (strain PA01). Infection models were treated with an NE inhibitor (sivelestat) before vABN breath tests to determine specificity of reporter release by NE (mean ± s.d., $n = 4$ or 5 mice per group, one-way ANOVA with Tukey's multiple comparisons test, ***$p = 0.0006$, ****$p < 0.0001$, n.s. = not significant where $p = 0.1681$).

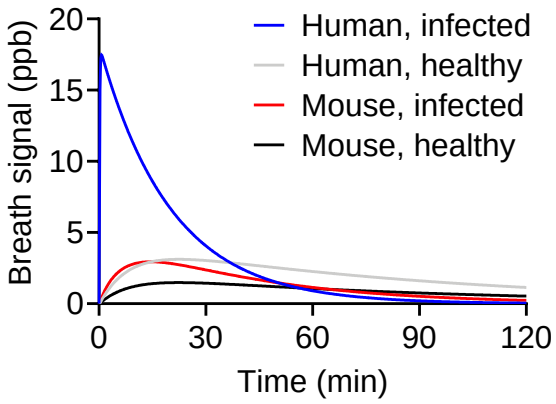

Supplementary Figure 13. Prediction of human breath signal during lung infection using the PBPK model. Human-specific values for parameters such as human equivalent vABN dose, neutrophil elastase concentrations during lung infection, and minute and tidal volumes during respiration were used in the PBPK model to predict breath signal in healthy humans and humans with lung infection. Mouse breath signal predictions are included for comparison.

Supplementary References

1. Kwon, E. J., Dudani, J. S. & Bhatia, S. N. Ultrasensitive tumour-penetrating nanosensors of protease activity. *Nat. Biomed. Eng.* **1,** (2017).

2. Kwong, G. A., Dudani, J. S., Carrodeguas, E., Mazumdar, E. V & Zekavat, S. M. Mathematical framework for activity-based cancer biomarkers. *PNAS* **112,** 21–24 (2015).

3. Gursahani, H., Riggs-sauthier, J., Pfeiffer, J. & Lechuga-ballesteros, D. Absorption of polyethylene glycol (PEG) polymers : The effect of PEG size on permeability. *J. Pharm. Sci.* **98,** 2847–2856 (2009).

4. Korfhagen, T. R. *et al. Altered surfactant function and structure in SP-A gene targeted mice*. *Cell Biology* **93,** (1996).

5. Lin, Y.-W. *et al.* Pharmacokinetics/Pharmacodynamics of Pulmonary Delivery of Colistin against Pseudomonas aeruginosa in a Mouse Lung Infection Model. (2017). doi:10.1128/AAC.02025-16

6. Michael J. Derelanko, M. A. H. *Handbook of Toxicology*. (CRC Press/Taylor and Francis, 2002).

7. Rennard, S. I. *et al. Estimation of volume of epithelial lining fluid recovered by lavage using urea as marker of dilution*.

8. Ng, A. W., Bidani, A. & Heming, T. A. Innate host defense of the lung: Effects of lung-lining fluid pH. *Lung* **182,** 297–317 (2004).